Journal of Hazardous Materials 192 (2011) 620–627

Contents lists available at ScienceDirect

Journal of Hazardous Materials

journal homepage: www.elsevier.com/locate/jhazmat

Synthesis and characterization of monodispersed orthorhombic manganese oxide nanoparticles produced by *Bacillus* sp. cells simultaneous to its bioremediation

Arvind Sinha [a], Vidya Nand Singh [b], Bodh Raj Mehta [b], Sunil Kumar Khare [a,*]

[a] Enzyme and Microbial Biochemistry Laboratory, Department of Chemistry, Indian Institute of Technology, Delhi, Hauz Khas, New Delhi 110 016, India
[b] Thin Film Laboratory, Department of Physics, Indian Institute of Technology, Delhi Hauz Khas, New Delhi 110016, India

ARTICLE INFO

Article history:
Received 17 February 2011
Received in revised form 19 May 2011
Accepted 20 May 2011
Available online 6 June 2011

Keywords:
Manganese oxide nanoparticle
Manganese bioremediation
Bacillus sp.
Nanoparticle synthesis
Orthorhombic manganese oxide

ABSTRACT

A heavy metal resistant strain of *Bacillus* sp. (MTCC10650) is reported. The strain exhibited the property of bioaccumulating manganese, simultaneous to its remediation. The nanoparticles thus formed were characterized and identified using energy dispersive X-ray analysis (EDAX), high resolution transmission electron microscopy (HRTEM), X-ray photoelectron spectroscopy (XPS), powder X-ray diffraction (PXRD) and atomic force microscopy (AFM). When the cells were challenged with manganese, the cells effectively synthesized nanoparticles of average size 4.62 ± 0.14 nm. These were mostly spherical and monodispersed. The ex situ enzymatically synthesized nanoparticles exhibited an absorbance maximum at 329 nm. These were more discrete, small and uniform, than the manganese oxide nanoparticles recovered after cell sonication. The use of *Bacillus* sp. cells seems promising and advantageous approach. Since, it serves dual purposes of (i) remediation and (ii) nanoparticle synthesis. Considering the increasing demand of developing environmental friendly and cost effective technologies for nanoparticle synthesis, these cells can be exploited for the remediation of manganese from the environment in conjunction with development of a greener process for the controlled synthesis of manganese oxide nanoparticles.

1. Introduction

Synthesis of nanosize manganese oxide particles has attracted special attention because of their unique physical and chemical properties. The manganese nanoparticles have copious industrial applications in supercapacitors, catalysis, biosensors, ion sieves, molecular adsorption, high density magnetic storage media, batteries, drug delivery system and magnetic resonance imaging [1–6]. Since, the properties of nanoparticles are size and shape dependent, the synthesis process having good control on monodispersity, size and shape is an important area of research [7]. Currently, different chemical and physical methods are employed for the synthesis of nanosize manganese oxide particles. Most of these techniques require stringent reaction conditions, viz very high temperature, pressure and the use of toxic chemicals [8–10]. Also, a strong tendency to precipitate or coagulate during the synthesis renders the processes more difficult [11–14].

Biological systems have well organized and controlled physiological processes and thus, their use in the nanoparticle synthesis is rapidly gaining importance. Several strains of microorganisms are known for having metal resistance capability. They are endowed with various cellular mechanisms for metal detoxification. The synthesis of nanosized metal is one such strategy/adaptive feature [15,16]. The use of microbial systems in nanobiosynthesis have been successfully demonstrated for gold nanoparticles by *Bacillus subtilis*, *Pseudomonas* sp., *Verticellum* and *Fusarium* sp., silver nanoparticles by *Bacillus* sp., Fe_3O_4 magnetic nano crystals by *Magnetospirillum magnetotacticum*, palladium nanoparticle by sulphate reducing bacteria [17] and CdS nano crystals by *Rhodobacter spheroids* [18]. Microbes are therefore, amenable to be exploited, for the synthesis of nanoparticles with controlled shape, size and monodispersity [19].

In nature, the excess of Mn^{2+} is oxidized by both abiotic and biotic processes. The formation of Mn^{3+} and Mn^{4+} is thermodynamically favorable in the presence of oxygen and higher pH. Nevertheless, these are mostly catalyzed by microorganisms due to the higher activation energy [20]. Microbial systems, especially bacterial like *Pseudomonas putida* strains MnB1, *Bacillus* sp. SG-1, *Leptothrix discophora* SP-6 and *Leptothrix discophora* SS-1 have been used as attractive model systems for the microbial manganese oxidation [21]. However, these strains have rarely been exploited for the synthesis of manganese oxide nanoparticles [22].

Manganese rich discharge is one of the major constituent of industries involving steel and nonsteel alloy production, colorants, pigments, battery manufacture, fuel additives, catalysts, and metal coatings. Manganese at higher concentration is neurotoxic; causing neurological syndrome like Parkinson's disease [23,24]. Therefore

* Corresponding author. Tel.: +91 11 26596533; fax: +91 11 26581102.
E-mail addresses: skhare@rocketmail.com, skkhare@chemistry.iitd.ac.in (S.K. Khare).

0304-3894/$ – see front matter © 2011 Elsevier B.V. All rights reserved.
doi:10.1016/j.jhazmat.2011.05.103

microbial systems having manganese bioaccumulating properties may be advantageous to serve two purposes (i) remediation and (ii) nanoparticle synthesis.

Taking advantage of the manganese bioaccumulating potential of the self isolated *Bacillus* sp. strain, the present work explores the feasibility of manganese remediation simultaneous to the synthesis of manganese oxide nanoparticles as a model system.

2. Materials and methods

2.1. Materials

$MnCl_2.4H_2O$ was a procured from Glaxo Laboratories Ltd. (Mumbai, India). The media components were procured from Hi Media Laboratories (Mumbai, India). All other chemicals used were of analytical grade. A stock solution of 1000 mg L^{-1} $MnCl_2{\cdot}4H_2O$ was prepared in Milli Q water and 0.22 μ filter sterilized $MnCl_2{\cdot}4H_2O$ solution equivalent to the respective manganese concentration was used in each experiment.

2.2. Bacterial strain and culture conditions

A metal resistant *Bacillus* sp. strain, isolated from soil was used in the present study. The samples were obtained from oil spilled soil near about IIT Delhi (India). The strain was isolated and purified by repeated streaking on nutrient agar plates. It was identified by morphological, biochemical and 16S rDNA analysis. The 16S rDNA sequence was submitted to National Center for Biotechnology Information GenBank, NCBI, USA. The NCBI GenBank accession number assigned is JF281096. The pure culture was submitted to Microbial Type Culture Collection, IMTECH Chandigarh, India, with accession no. MTCC 10650. The culture was maintained at 4 °C in agar slants and sub-cultured at monthly intervals. The purity of the laboratory culture was checked at regular time intervals by repeated streaking on nutrient agar plates.

2.2.1. Inoculum

A loopful of inoculum from the slant was introduced into the mother culture medium containing (g L^{-1}): yeast extract 3.0; peptone, 5.0; NaCl, 2.5; adjusted to pH 7.0 followed by incubation at 30 °C and 120 rpm. The 24 h grown culture having OD ~ 1.0 (A_{660} nm) was used as the mother culture.

2.2.2. Culture conditions

50 mL of culture medium containing (g L^{-1}): yeast extract, 3.0; peptone, 5.0; glucose, 5.0; NaCl, 2.5; $MgSO_4{\cdot}7H_2O$, 0.5; pH 7.5 was taken in a 250 mL Erlenmeyer flask. The culture medium was inoculated with 1% (v/v) mother culture and incubated at 30 °C with constant shaking at 120 rpm (Orbital Rotary Shaker, Orbitech, India). The culture medium composition and conditions were kept parallel in all the experiments otherwise stated. Growth of the cells was recorded at 660 nm using double beam UV–visible spectrophotometer (Specord 200, Analytikjena, Germany).

2.3. Biosynthesis of manganese oxide nanoparticles

Predetermined concentrations (as per the experimental conditions) of filter sterilized $MnCl_2{\cdot}4H_2O$ was added into the culture medium prior to inoculation. Rest of the culture conditions were kept same as described in Section 2.2.2. The samples were withdrawn periodically and processed accordingly for monitoring (i) the cell growth (ii) manganese concentration (iii) nanoparticle synthesis. Five millilitres of culture media was withdrawn aseptically at regular time intervals and centrifuged at 14,000 × *g* for 10 min at 4 °C. The supernatant was taken to estimate the residual manganese by using atomic absorption spectrophotometer (AAnalyst 100, Perkin-Elmer, USA). A part of the culture was further processed for the transmission electron microscopy. A control experiment was similarly run without inoculating with the cells to check for any abiotic precipitation of the manganese during the operational experimental conditions.

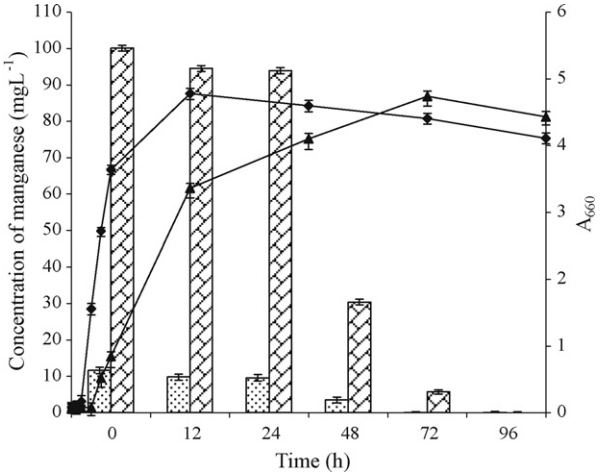

Fig. 1. Growth and manganese bioremediation by *Bacillus* sp. cells. The cells were grown in culture medium as described in materials and methods Section 2.3; [♦], bacterial growth (A_{660}) in presence of 10 mg L^{-1} manganese; [▲], bacterial growth (A_{660}) in presence of 100 mg L^{-1} manganese; [▨], residual manganese concentration in culture media (10 mg L^{-1} manganese); [▨], residual manganese concentration in culture media (100 mg L^{-1} manganese).

2.4. Effect of varying culture conditions on nanoparticle synthesis

Cells were cultivated as described in Section 2.3, except that one parameter was varied at a time. For incubation time, the cells grown in 100 mg L^{-1} manganese were harvested at different time intervals of 24, 48 and 72 h. The effect of manganese concentration was monitored at 100 mg L^{-1}, 150 mg L^{-1} or 200 mg L^{-1} manganese. The cells were harvested after 72 h of incubation. The harvested cells with different culture conditions were analyzed by transmission electron microscopy.

2.5. Analytical methods used for identification and characterization of synthesized nanoparticles

2.5.1. Transmission electron microscopy (TEM)

Cells grown in absence or presence of manganese were harvested by centrifugation at 8000 × *g* for 10 min at 4 °C. The pellets were washed thrice with phosphate buffer (0.1 M, pH 7.4) and fixed overnight in modified Karnovsky's fluid at 4 °C. Post fixation was done with 1% OsO_4 for 1 h at room temperature. Dehydration was carried out with acetone series (30, 50, 70, 90 and 100% acetone). The samples were treated for 30 min at each acetone concentrations and processed further as per the procedure of David et al. [25]. Transmission electron micrographs were recorded without regular double staining in TEM equipped with EDAX (HRTEM, Technai G^2; 200 kV, USA). High resolution transmission electron microscopy (HRTEM) and energy dispersive X-ray analysis was done on the same bacterial thin film used for taking TEM micrographs in nanoprobe mode.

2.5.2. X-ray photoelectron spectroscopy (XPS)

In a 250-mL Erlenmeyer flask, 50 mL of culture medium containing 100 mg L^{-1} manganese was inoculated and incubated as

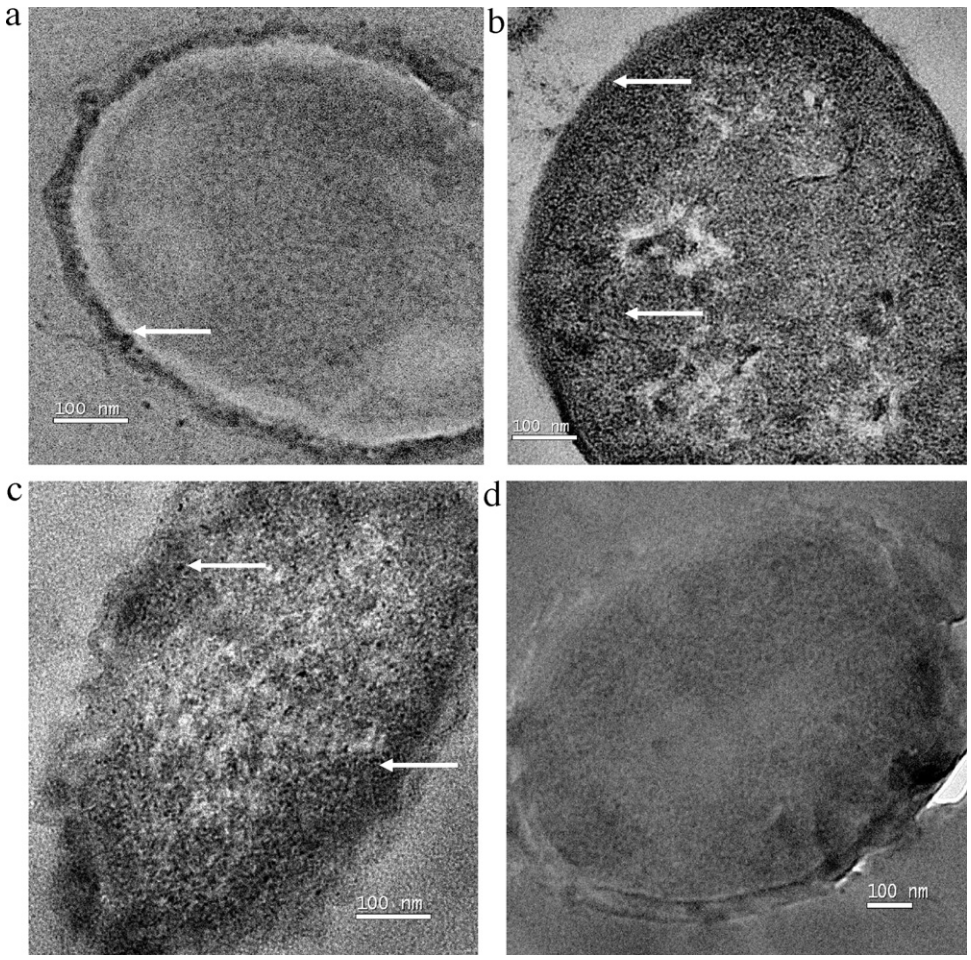

Fig. 2. Transmission electron micrograph (TEM) of *Bacillus* sp. cells taken at different time of growth. The cells were grown in culture medium as described in Section 2.4; cell grown in manganese for (a) 24 h; (b) 48 h; (c) 72 h; (d) control, cells grown in absence of manganese for 72 h. Arrow heads show manganese oxide accumulation. Bar scale 100 nm.

described in Section 2.2.2. After 72 h of incubation, the cells were harvested by centrifugation at 14,000 × *g* for 10 min at 4 °C. The pellet was washed thrice with Milli Q water and finally resuspended in 500 μL of Milli Q water. The resuspended cells were sonicated (A) at a frequency 24 kHz for 10 min under ice cold conditions. The sonicated culture was spreaded uniformly over a glass cover slip coated with 0.5% gelatin and dried at room temperature. X-ray photoelectron spectroscopy (XPS) was performed on Specs (SPECS GmbH, Berlin, Germany). The photoelectrons were excited using an MgK*α* source of energy 1253.6 eV. The accuracy in the binding energy determination was 0.05 eV. The spectra obtained were calibrated to the binding energy (BE) of C1s at 284.6 eV to compensate the surface charging effect.

2.5.3. Powder X-ray diffraction (PXRD)

A part of the sonicated cells (A) as obtained in Section 2.5.2 was lyophilized and crushed into fine powder and subjected to powder XRD (D2 Phaser, Bruker, Germany).

2.5.4. Fourier transform infrared (FT-IR) characterization

The fine powder as obtained in Section 2.5.3 was also analyzed by Fourier transform infrared spectroscopy. The spectra were recorded in range of 400–4000 cm^{-1} on Nicolet 6700 FT-IR (Thermo Scientific, USA) using KBr.

2.5.5. Possible recovery of manganese oxide and high resolution transmission electron microscopy (HRTEM) of cell lysate

Cells grown for 72 h were pelleted and washed with Milli Q water as described in Section 2.5.2. These were finally resuspended in 1 mL of Milli Q water and sonicated at a frequency 24 kHz for 10 minutes under ice cold condition followed by filtration through a 0.45 μ Millipore filter. One drop of filtered lysate was loaded on a carbon coated grid, dried at room temperature and subjected to TEM/HRTEM analysis.

2.5.6. Atomic force microscopy (AFM)

The filtered (0.45 μ) lysate as obtained in Section 2.5.2 was spreaded uniformly on a thin glass plate and dried at room temperature. The AFM images were recorded on the AFM system (Nanoscope IIIa; Vecco Metrology Group, Santa Barbara, CA, USA) with a scan rate of about 10.17 Hz.

2.6. Ex situ synthesis of manganese oxide nanoparticle by cell extract of Bacillus sp. and their TEM, UV–visible characterization

In a 500-mL Erlenmeyer flask, 100 mL of culture medium was inoculated and incubated as described in Section 2.2.2. After 72 h of incubation, cells were harvested by centrifugation at 14,000 × *g* for 10 min at 4 °C. The pellets were washed thrice with 10 mM HEPES buffer, pH 7.5 and finally resuspended in 2 mL of 10 mM HEPES buffer. These were sonicated at a frequency 24 kHz for 10 min

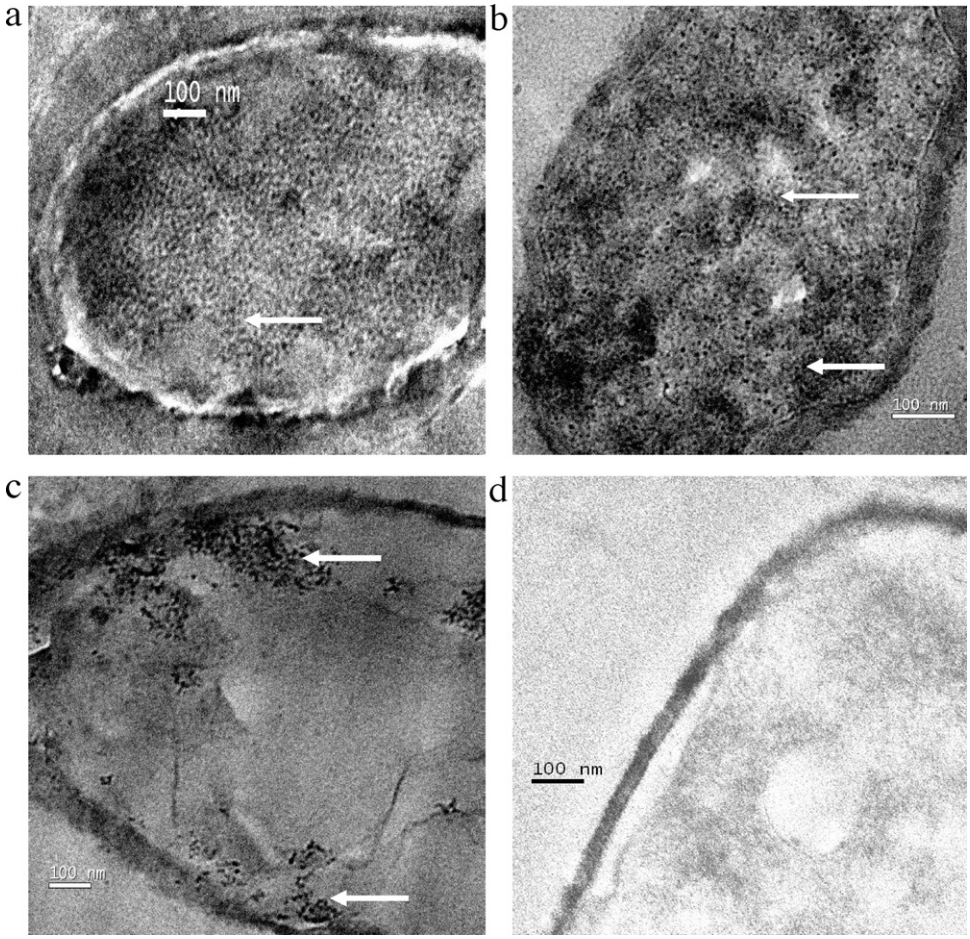

Fig. 3. Effect of manganese concentration in media on synthesis of manganese oxide nanoparticles by *Bacillus* sp. cells. The cells were grown in culture medium as described in Section 2.4; (a) 100 mg L^{-1}; (b) 150 mg L^{-1}; (c) 200 mg L^{-1}; (d) control, cells grown in absence of manganese. Arrow heads show manganese oxide accumulation. Bar scale 100 nm.

followed by centrifugation at 8000 × *g* for 10 min at 4 °C. Two millilitres of the supernatant cell lysate was collected and incubated with 100 μM $MnCl_2$ at 30 °C and 120 rpm in Orbitek shaker. The manganese oxide synthesis was routinely monitored by recording the UV–visible spectra. One drop of the 72 h incubated and filtered (0.45 μ) lysate was loaded on a carbon coated grid, dried at room temperature and examined under TEM.

All the experiments were performed in triplicate and variation was within ± 5%.

3. Results and discussion

3.1. Manganese remediation and localization of nanoparticles

In order to evaluate the manganese bioremediation potential of the *Bacillus* sp. cells, the residual manganese concentration in the culture media was estimated at different time intervals. Fig. 1 shows the growth profile and residual manganese concentration in the culture medium as a function of time. The initial load of 100 mg L^{-1} manganese from the culture medium was completely remediated in 96 h whereas complete remediation of low concentration load (10 mg L^{-1} manganese) was achieved in 72 h. As per the growth curve and manganese remediation patterns, it is evident that most of the manganese was remediated during the late exponential phase of the cells growth. These results are supported by previous studies on manganese oxidizing strains which oxidize manganese during their stationary phase [20]. In control experiment there was no significant decrease in manganese concentration (data not shown). It is known that different mechanisms of metal detoxification and uptake could operate simultaneously or individually in a microbial system depending on the environmental conditions [26]. The microbial systems according to their adaptive and physiological mechanisms can detoxify the metal by (i) effluxing it out (ii) accumulating in the cytoplasm or by (iii) converting it into less toxic form. Thus, it is quite possible that during the late exponential phase of the growth some cellular mechanism has been triggered, which might have facilitated the entry of manganese inside the cells. Nevertheless, the exact mechanism of the manganese uptake by the *Bacillus* sp. cells under investigation is yet to be fully understood.

To comprehend the fate of the remediated manganese, whether it was precipitated out or accumulated inside the cells, transmission electron micrographs of the cells harvested at different time intervals were recorded (Fig. 2). Cells grown for 24 h (Fig. 2(a)) showed very few, small sized and randomly dispersed particles on the cell wall only. Proliferation of accumulated manganese in the cytoplasm was seen in 48 h (Fig. 2(b)) and 72 h (Fig. 2(c)) grown cells. The accumulated particles were spherical and uniformly dispersed into the cytoplasm. The majority of the accumulated particles were less than 6 nm in diameter. The corresponding control, cells grown in absence of manganese for 72 h is shown in Fig. 2(d) for comparison. Thus, it is logical to conclude from the bioremediation profile and TEM micrographs that the process of manganese uptake from

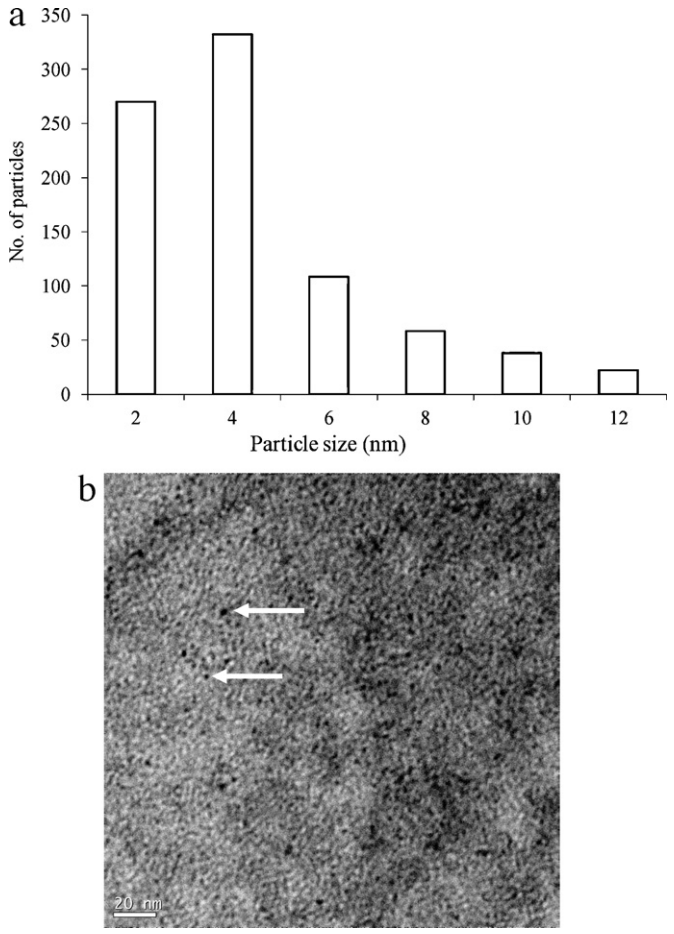

Fig. 4. A particle size distribution histogram and TEM micrograph at higher magnification. (a) Particle size distribution histogram, as determined from the TEM micrograph; (b) TEM micrograph of cell grown in presence of 150 mg L^{-1} manganese. Arrow heads show manganese oxide accumulation. Bar scale 20 nm.

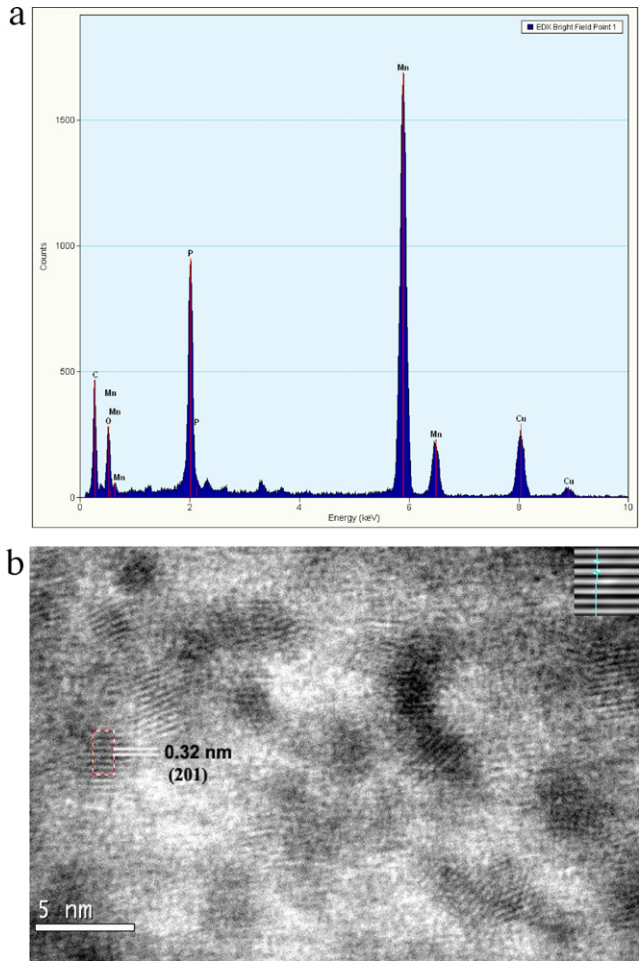

Fig. 5. Energy dispersive X-ray (EDAX) profile and high resolution transmission electron microscopy (HRTEM) image of *Bacillus* sp. cells grown in presence of 100 mg L^{-1} manganese. (a) EDAX profile; (b) HRTEM image. EDAX and HRTEM were performed on the same bacterial thin films which were used for recording TEM micrographs.

the medium and synthesis of nanoparticles took place during the late exponential growth phase of the cells.

Metal bioaccumulation is a well documented phenomenon among many microorganisms viz. Cr (IV), Pb (II), Cu (II) in *Aspergillus niger* [27], Ni by *Pseudomonas* sp. [28], Ag by *Bacillus* sp. and several others [29]. The interesting observation was that the *Bacillus* sp. strain under investigation, formed manganese oxide nanoparticles simultaneous to its remediation. This seems to be a doubly useful approach that a microorganism is synthesizing nanoparticles from the metal being remediated by it. The synthesis of nanosize manganese oxide particles around the metal center inside the cells could be mediated through some oxidase enzyme followed by aggregation with other cellular proteins.

3.2. Effect of manganese concentration on the nature of nanoparticles

The cells were subjected to an increasing amount of manganese in the culture medium. The representative TEM micrographs (Fig. 3) showed that the nanoparticles synthesized by the cells at, 100 mg L^{-1} (Fig. 3(a)) and 150 mg L^{-1} (Fig. 3(b)) manganese concentration were similar in morphology and distribution while the cells treated with 200 mg L^{-1} manganese (Fig. 3(c)) showed alignment of particles mostly near the cell wall. The TEM micrograph of corresponding control is shown in Fig. 3(d).

The particle size distribution histogram (Fig. 4(a)) as determined from the transmission electron micrograph showed that the average size of the particles under investigation were 4.6 ± 0.14 nm, with some particles, having 6–8 nm size and a very small percentage having diameter greater than 10 nm. In general, the particles were isotropic in nature and monodispersed without any agglomeration. This was further confirmed by the TEM micrograph of the cell taken at higher magnification (Fig. 4(b)). The *Bacillus* sp. system thus proves to be a fairly good one for the synthesis of monodispersed nanoparticles.

3.3. Characterization and identification of accumulated nanoparticles

The bio-accumulation of manganese evident in the transmission electron micrographs of the cells was further confirmed by EDAX profiling of the manganese bioaccumulating cells (Fig. 5(a)). Signals in EDAX at 5.89 keV and 6.49 keV can be attributed to manganese (Mn) Kα and the secondary (Mn) K_β peaks respectively, which prove that the accumulated particles were indeed manganese. The high resolution transmission electron micrograph (HRTEM) image provides further insight into the structure of the intracellularly synthesized nanoparticles (Fig. 5(b)). The image exhibits lattice fringes with *d* spacing of 0.32 nm, which is consistent with the 0.32 nm separation between the 201 planes of manganese oxide which was further confirmed by the powder XRD pattern (Fig. 6).

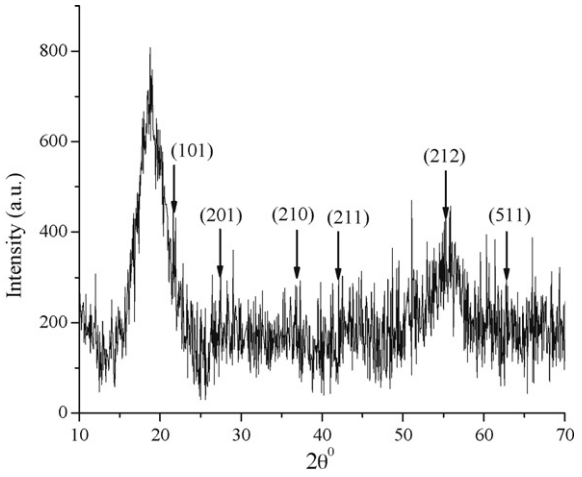

Fig. 6. The powder XRD patterns of *Bacillus* sp. cells grown in presence of 100 mg L^{-1} manganese for 72 h.

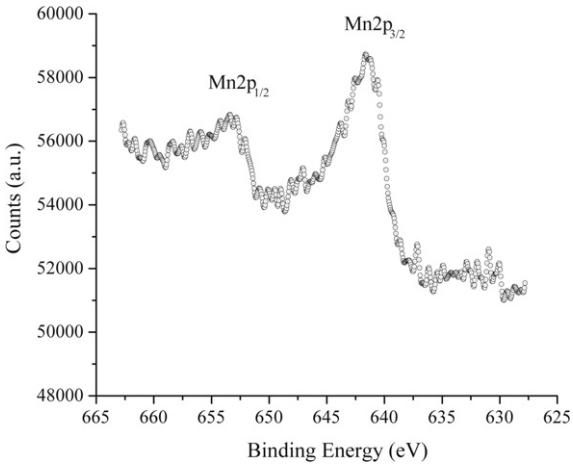

Fig. 7. X-ray photoelectron spectral profile of *Bacillus* sp. cells grown in presence of 100 mg L^{-1} manganese for 72 h as described in Section 2.5.2.

Inspite of a strong background scattering from the organic and inorganic components of the cells, weak diffraction peaks at *d* values 0.407, 0.324, 0.243, 0.214, 0.165 and 0.147 can be recognized and can be assigned to the reflections (1 0 1), (2 0 1), (2 1 0), (2 1 1), (2 1 2) and (5 1 1) of MnO_2 (JCPDS # 39-0375). Both the HRTEM and the XRD profiles of the manganese oxide nanoparticles present in intact cytoplasm were consistent and confirmed the formation of orthorhombic MnO_2.

In order to probe the oxidation state, the intracellularly synthesized nanoparticles were further characterized, by XPS. The Mn 2p core level spectrum recorded on the sonicated cell lysate is shown in Fig. 7. Because of heterogeneous nature of the cells, strong background scattering from the other organic cell components takes place. This along with the smaller binding energy difference (~2 eV) between the different oxidation states make it difficult to speciate the particular oxidation state of the manganese on the cell lysate. However, the comparison of the measured binding energy for $Mn(2p_{3/2})$ and $Mn(2p_{1/2})$ transitions centered at 641.65 and 653.45 eV respectively having spin energy separation of 11.80 eV in the present work with the values available in the literature, indicated the presence of manganese as Mn^{4+} [30–32] which is consistent with the oxidation state of Mn in MnO_2.

More characteristics of MnO_2 were observed in its FTIR spectrum (Fig. 8). The bands around 1548, 1400 and 1030 cm^{-1} can be attributed to O–H bending vibrations combined with Mn atoms [33]. The intense band observed around 590 cm^{-1} could be attributed to the Mn–O vibrations in MnO_6 octahedra [34]. The presence of a broad band at about 3302 cm^{-1} and 1651 cm^{-1} indicate the presence of few bound water molecules in the MnO_2 samples [35].

Thus, it can be concluded from the various analytical results that the intracellularly synthesized nanoparticles were orthorhombic MnO_2.

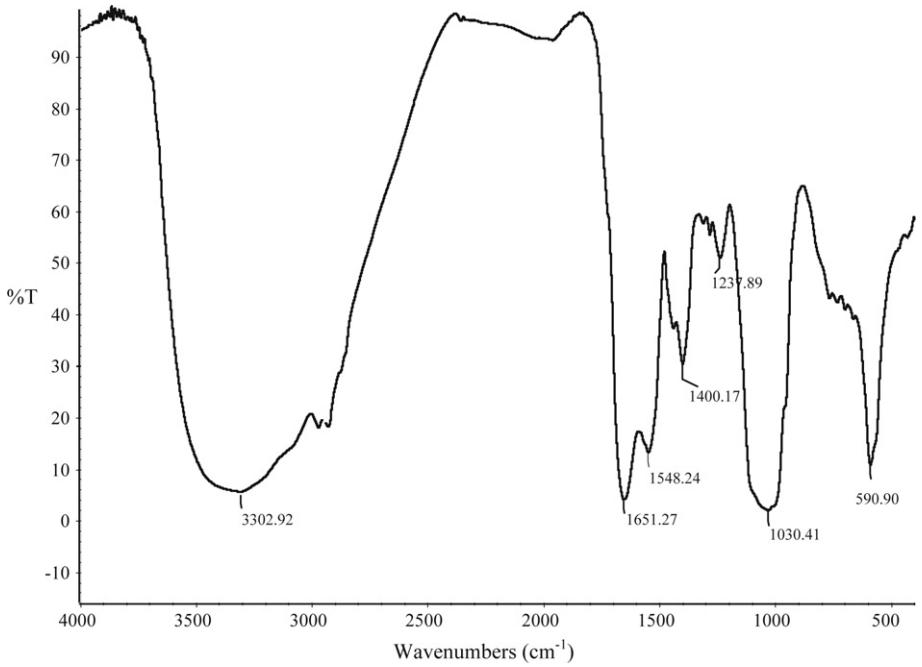

Fig. 8. FT-IR spectra of *Bacillus* sp. cells grown in presence of 100 mg L^{-1} manganese for 72 h described in Section 2.5.4.

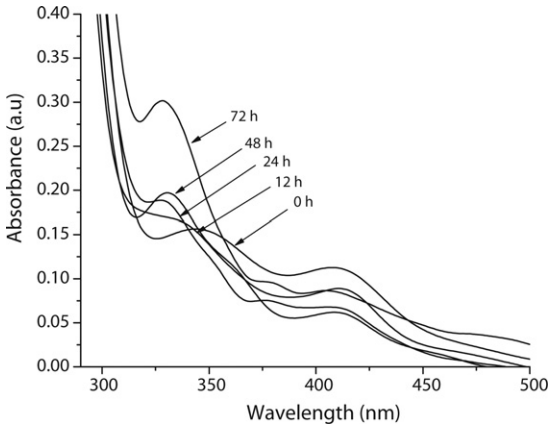

Fig. 9. UV–visible absorption spectra of ex situ synthesis of manganese oxide nanoparticle by *Bacillus* sp. cell extract as a function of time. Two millilitre of *Bacillus* sp. cell extract as prepared in Section 2.6 was incubated with 100 μM $MnCl_2$ at 30 °C and 120 rpm. UV–visible absorption spectrum was recorded for the samples withdrawn at different time intervals.

3.4. Ex situ synthesis and recovery of manganese oxide nanoparticles by cell sonication

The ex situ synthesis of manganese dioxide was monitored by using UV–visible absorption spectroscopy. A broad absorbance band with a maximum at 329 nm can be observed (Fig. 9), which progressively increases in intensity as the reaction/synthesis progresses from 0 h to 72 h. The absorbance occurred at a lower wavelength than that observed for bulk manganese oxide which is consistent with quantum confinement due to the small particle size [36]. The increase in intensity with no appreciable shift in the absorption maxima with the progress of time was observed. This suggests that the size of the particles remained almost same, while the number of particles increased. This also supplemented the results obtained in the TEM micrographs.

To assess the feasibility of recovering the intracellularly synthesized manganese oxide nanoparticles and to compare them with those synthesized by cell extract, the cells containing intracellular nanoparticles were subjected to ultrasonication. Fig. 10(a) and (b) shows the TEM micrographs of nanoparticles synthesized by cell extract and those synthesized intracellularly by the cells. The cell extract synthesized nanoparticles were more discrete, small and uniform, than the recovered manganese oxide nanoparticles.

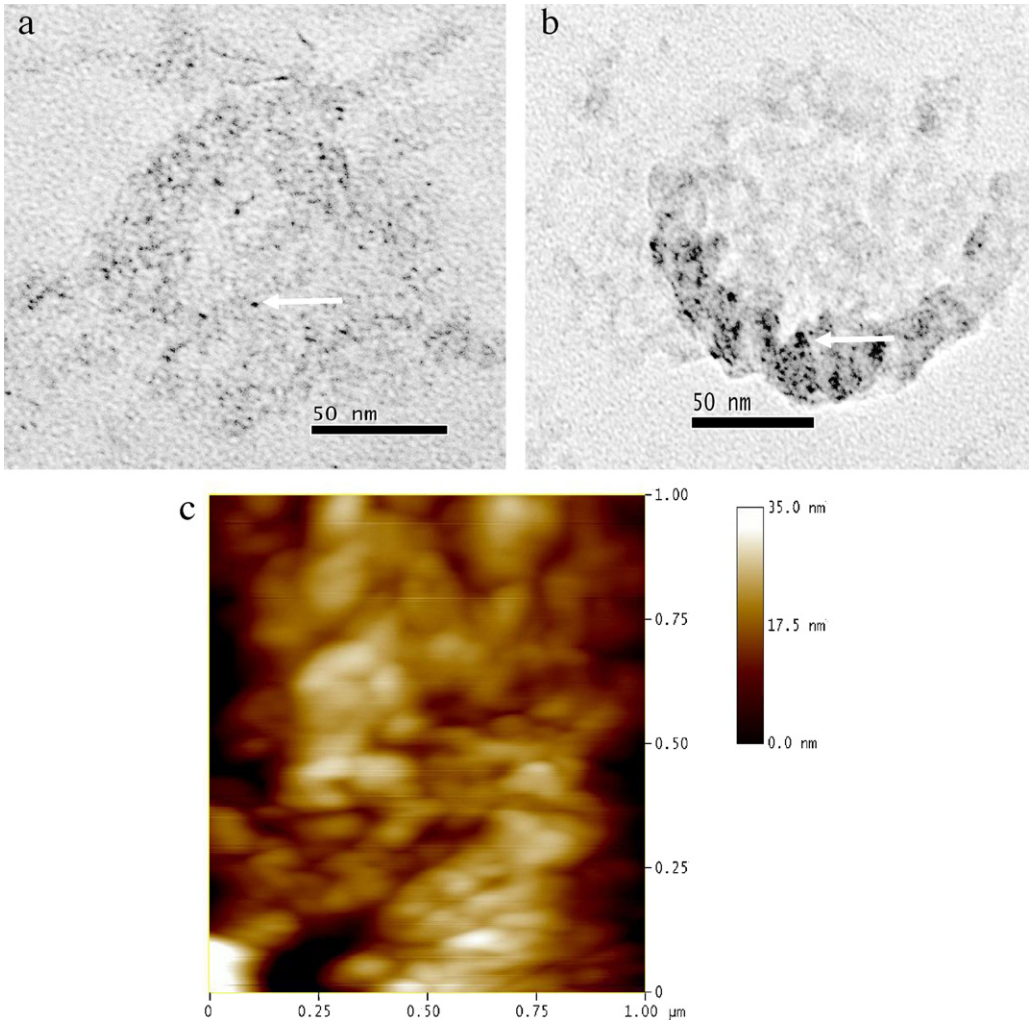

Fig. 10. TEM, AFM analysis of (i) ex situ synthesized manganese oxide nanoparticle from the cell extract and (ii) Intracellular synthesized manganese oxide nanoparticles recovered after cell sonication. (a) TEM of cell extract treated with 100 μM $MnCl_2$ at 30 °C and 120 rpm for 72 h (b) TEM of cell lysate showing recovered nanoparticles after cell sonication. Arrow head shows manganese oxide nanoparticles. Bar scale 50 nm. (c) AFM roughness analysis of the recovered nanoparticles.

Fig. 10(c) shows the AFM analysis of the recovered nanoparticles. The mean roughness as observed was found to be 5.47 nm. The recovered nanoparticles were spherical and uniform in shape as evident from the AFM profile. The possibility of recovering the intracellularly synthesized and the ex situ enzymatically synthesized nanoparticles, further adjoin the usefulness and viability of the *Bacillus* sp. cells for manganese oxide nanobiosynthetic process.

4. Conclusions

The results demonstrate the feasibility of *Bacillus* sp. cells, to synthesize intracellular manganese oxide nanoparticles, while remediating manganese from the culture media, with good monodispersity. The synthesized nanoparticles were characterized as orthorhombic MnO_2. The intracellularly synthesized manganese oxide nanoparticles were recoverable. These particles can also be synthesized ex situ by the *Bacillus* sp. cell lysate. The study seeks to solve the environmental problem of manganese contamination, giving an advantage of biosynthesis of the corresponding oxide nanoparticles. The simplicity and a greener approach would make this process ideal for waste water treatment besides nanoparticle synthesis.

Acknowledgements

The research grant provided by the Department of Biotechnology (Govt. of India) for carrying out this study is gratefully acknowledged. Author Arvind Sinha is grateful to the University Grant Commission, New Delhi for the award of Senior Research Fellowship.

References

[1] B. Ammundsen, J. Paulsen, Novel lithium-ion cathode materials based on layered manganese oxides, Adv. Mater. 13 (2001) 943–956.
[2] B.J. Aronson, C.F. Blanford, A. Stein, Synthesis, characterization, and ion-exchange properties of zinc and magnesium manganese oxides confined within MCM-41 channels, J. Phys. Chem. B 104 (2000) 449–459.
[3] Y.Q. Chang, X.Y. Xu, X.H. Luo, C.P. Chen, D.P. Yu, Synthesis and characterization of Mn_3O_4 nanoparticles, J. Cryst. Growth 264 (2004) 232–236.
[4] X. Fu, J. Feng, H. Wang, K.M. Ng, Room temperature synthesis of a novel γ-MnO_2 hollow structure for aerobic oxidation of benzyl alcohol, Nanotechnology 20 (2009) 1–9.
[5] J. Shin, R.M. Anisur, M.K. Ko, G.H. Im, J.H. Lee, I.S. Lee, Hollow manganese oxide nanoparticles as multifunctional agents for magnetic resonance imaging and drug delivery, Angew. Chem. Int. Ed. 48 (2009) 321–324.
[6] A.A. Gilad, P. Walczak, M.T. McMahon, H.B. Na, J.H. Lee, K. An, T. Hyeon, P.C.M. Van Zijl, J.W.M. Bulte, MR tracking of transplanted cells with "positive contrast" using manganese oxide nanoparticles, Magn. Reson. Med. 60 (2008) 1–7.
[7] Y. Sun, Y. Xia, Shape-controlled synthesis of gold and silver nanoparticles, Science 298 (2002) 2176.
[8] H. Men, P. Gao, Y. Sun, Y. Chen, X. Wanga, L. Wanga, Synthesis of nanostructured manganese oxides from a dipolar binary liquid (water/benzene) system and hydrogen storage ability research, Int. J. Hydrogen Energy 35 (2010) 9021–9026.
[9] N. Pinna, M. Niederberger, Surfactant-free nonaqueous synthesis of metal oxide nanostructures, Angew. Chem. Int. Ed. 47 (2008) 5292–5304.
[10] Y. Wang, J. Zhu, J. Han, R. Guo, Modification of MnO_2 nanoparticles with rutin synthesized by Triton X-100 aggregations' template, Nanotechnology 19 (2008) 1–8.
[11] T.D. Schladt, T. Graf, W. Tremel, Synthesis and characterization of monodisperse manganese oxide nanoparticles-evaluation of the nucleation and growth mechanism, Chem. Mater. 21 (2009) 3183–3190.
[12] I. Djerdj, D. Arcon, Z. Jaglicic, M. Niederberger, Nonaqueous synthesis of manganese oxide nanoparticles, structural characterization, and magnetic properties, J. Phys. Chem. C 111 (2007) 3614–3623.
[13] L.-X. Yang, Y.J. Zhu, H. Tong, W.W. Wang, G.F. Cheng, Low temperature synthesis of Mn_3O_4 polyhedral nanocrystals and magnetic study, J. Solid State Chem. 179 (2006) 1225–1229.
[14] Y.C. Zhang, T. Qiao, X.Y. Hu, Preparation of Mn_3O_4 nanocrystallites by low-temperature solvothermal treatment of γ-MnOOH nanowires, J. Solid State Chem. 177 (2004) 4093–4097.
[15] M. Gericke, A. Pinches, Biological synthesis of metal nanoparticles, Hydrometallurgy 83 (2006) 132–140.
[16] D. Mandal, M.E. Bolander, D. Mukhopadhyay, G. Sarkar, P. Mukherjee, The use of microorganisms for the formation of metal nanoparticles and their application, Appl. Microbiol. Biotechnol. 69 (2006) 485–492.
[17] K.B. Narayann, N. Sakthivel, Biological synthesis of metal nanoparticles by microbes, Adv. Colloid. Int. Sci. 156 (2010) 1–13.
[18] H. Bai, Z. Zhang, Y. Guo, W. Jia, Biological synthesis of size-controlled cadmium sulfide nanoparticles using immobilized *Rhodobacter sphaeroides*, Nanoscale Res. Lett. 4 (2009) 717–723.
[19] T.K. Joerger, R. Joerger, E. Olsson, C.G. Granqvist, Bacteria as workers in the living factory: metal-accumulating bacteria and their potential for materials science, Trends Biotechnol. 19 (2001) 15–20.
[20] B.M. Tebo, J.R. Bargar, B.G. Clement, G.J. Dick, K.J. Murray, D. Parker, R. Verity, S.M. Webb, Biogenic manganese oxides: properties and mechanisms of formation, Annu. Rev. Earth Planet. Sci. 32 (2004) 287–328.
[21] M. Villalobos, B. Toner, J. Bargar, G. Sposito, Characterization of the manganese oxide produced by *Pseudomonas putida* strain MnB1, Geochim. Cosmochim. Acta 67 (2003) 2649–2662.
[22] N. Miyata, Y. Tani, M. Sakata, K. Iwahori, Microbial manganese oxide formation and interaction with toxic metal ions, J. Biosci. Bioeng. 104 (2007) 1–8.
[23] S.M. Hussain, A.K. Javorina, A.M. Schrand, H.M. Duhart, S.F. Ali, J.J. Schlager, The interaction of manganese nanoparticles with PC-12 cells induces dopamine depletion, Toxicol. Sci. 92 (2006) 456–463.
[24] C.W. Olanow, Manganese-induced parkinsonism parkinson's disease, Ann. N.Y. Acad. Sci. 1012 (2004) 209–223.
[25] G.F.X. David, J. Herbert, G.D.S. Wright, The ultrastructure of the pineal ganglion in the ferret, J. Anat. 115 (1973) 79–97.
[26] B.M. Tebo, H.A. Johnson, J.K. McCarthy, A.S. Templeton, Geomicrobiology of manganese(II) oxidation, Trends Microbiol. 13 (2005) 421–428.
[27] A.Y. Dursun, G. Ulsu, Y. Cuci, Z. Aksu, Bioaccumulation of copper(II), lead(II) and chromium(VI) by growing *Aspergillus niger*, Process Biochem. 38 (2003) 1647–1651.
[28] T.M Roane, K.L. Josephson, I.L. Pepper, Dual-bioaugmentation strategy to enhance remediation of cocontaminated soil, Appl. Environ. Microbiol. 67 (2001) 3208–3215.
[29] K.N. Thakkar, S.S. Mhatre, R.Y. Parikh, Biological synthesis of metallic nanoparticles, Nanomedicine 6 (2010) 257–262.
[30] H.W. Nesbitt, D. Banerjee, Interpretation of XPS Mn(2p) spectra of Mn oxyhydroxides and constraints on the mechanism of MnO_2 precipitation, Am. Mineral 83 (1998) 305–315.
[31] B.V. Crist, Handbooks of Monochromatic XPS Spectra, The Elements and Native Oxides, XPS International, Inc, CA, 1999.
[32] B.J. Tan, K.J. Klabunde, P.M.A. Sherwood, XPS studies of solvated metal atom dispersed catalysts. Evidence for layered cobalt-manganese particles on alumina and silica, J. Am. Chem. Soc. 113 (1991) 855–861.
[33] M.V. Ananth, S. Pethkar, K. Dakshinamurthi, Distortion of MnO octahedra and electrochemical activity of Nstutite-based MnO polymorphs for alkaline electrolytes—an FTIR study, J. Power Sources 75 (1998) 278–282.
[34] C.M. Julien, M. Massot, C. Poinsignon, Lattice vibrations of manganese oxides part I. Periodic structures, Spectrochim. Acta Part A 60 (2004) 689–700.
[35] J. Ni, W. Lu, L. Zhang, B. Yue, X. Shang, Y. Lv, Low temperature synthesis of monodisperse 3D manganese oxide nanoflowers and their pseudocapacitance properties, J. Phys. Chem. C 113 (2009) 54–60.
[36] S.L. Brock, M. Sanabria, S.L. Suib, V. Urban, P. Thiyagarajan, D.I. Potter, Particle size control and self-assembly processes in novel colloids of nanocrystalline manganese oxide, J. Phys. Chem. B 103 (1999) 7416–7428.